Neurobiology of Disease 124 (2019) 240–247

Contents lists available at ScienceDirect

Neurobiology of Disease

journal homepage: www.elsevier.com/locate/ynbdi

High salt diet ameliorates functional, electrophysiological and histological characteristics of murine spontaneous autoimmune polyneuropathy

Petra Huehnchen[a,b,c,*], Wolfgang Boehmerle[a,b,c,1], Matthias Endres[a,b,c,d,e,f,1]

[a] Charité – Universitätsmedizin Berlin, Freie Universität Berlin, Humboldt-Universität zu Berlin, Berlin Institute of Health, Klinik und Hochschulambulanz für Neurologie, Berlin, Germany
[b] Charité – Universitätsmedizin Berlin, Freie Universität Berlin, Humboldt-Universität zu Berlin, Berlin Institute of Health, Cluster of Excellence NeuroCure, Berlin, Germany
[c] Berlin Institute of Health, 10178 Berlin, Germany
[d] Charité – Universitätsmedizin Berlin, Freie Universität Berlin, Humboldt-Universität zu Berlin, Berlin Institute of Health, Center for Stroke Resarch Berlin, Berlin, Germany
[e] German Center for Neurodegenerative Diseases (DZNE), Berlin, Germany
[f] DZHK (German Center for Cardiovascular Research), partner site Berlin, Berlin, Germany

ARTICLE INFO

Keywords:
Chronic inflammatory demyelinating polyradiculoneuropathy
Autoimmune neuropathy
High salt diet
Neuroinflammation
Demyelination

ABSTRACT

Background: It was previously reported that high salt dietary conditions can drive autoimmunity and worsen severity and symptoms of autoimmune diseases. Chronic inflammatory demyelinating polyradiculoneuropathy (CIDP) is a common autoimmune condition of the peripheral nervous system which leads to progressive paralysis and sensory deficits due to a demyelination and secondary axonal loss of peripheral nerves. We used a previously described model with a knockout of CD86 in non-obese diabetic mice ($CD86^{-/-}$ NOD), which results in the spontaneous development of an autoimmune peripheral neuropathy similar to CIDP and investigated the influence of a high salt diet on functional impairment, electrophysiological parameters, demyelination and neuroinflammation in these mice.

Methods: At seven weeks of age, asymptomatic female $CD86^{-/-}$ NOD mice were randomly assigned to a normal or high salt diet containing 4% sodium chloride in food and 1% in water. The diet was continued for a total of 30 weeks.

Results: Mice on the high salt diet showed a delayed onset of clinical symptoms and an ameliorated disease course with a reduced decline of locomotor function. Furthermore, electrophysiological parameters of neuropathy and demyelination were attenuated in mice on the high salt diet, which was confirmed with histological analysis. Additionally, we observed a reduced immune cell infiltration of sciatic nerves in mice which had received the high salt diet.

Conclusions: We demonstrate beneficial effects of high salt diet regarding disease progression, functional, electrophysiological and histological parameters in a transgenic mouse model of spontaneous autoimmune neuropathy.

1. Introduction

Chronic inflammatory demyelinating polyradiculoneuropathy (CIDP) is an autoimmune condition of the peripheral nervous system. It leads to severe paresis and sensory loss due to a progressive demyelination and secondary axonal loss of peripheral nerves (Reynolds et al., 2016). The underlying pathophysiology of CIDP is still largely unknown, but there is evidence for both the involvement of cell-mediated and humoral mechanisms. The significance of pathogenic autoantibodies against myelin proteins is underlined by beneficial responses of CIDP patients to plasmapheresis or treatment with intravenous immunoglobulins (IVIg) (Delmont et al., 2017; Kleyman and Brannagan 3rd, 2015). The relevance of cellular immune mechanisms in CIDP was proven by immune cell infiltrates in nerve biopsies of CIDP patients (Vital et al., 2000). Additionally, elevated expressions of pro-inflammatory cytokines were found in the cerebral spinal fluid of CIDP patients (Bonin et al., 2018) and the adoptive transfer of pathogenic T cells results in the development of CIDP-like symptoms and histopathological features in animal studies (Meyer Zu Horste et al., 2014; Salomon et al., 2001). The secretion of pro-inflammatory cytokines by

* Corresponding author at: Charité Universitätsmedizin Berlin, Klinik für Neurologie, Charitéplatz 1, Berlin 10117, Germany.
E-mail address: petra.huehnchen@charite.de (P. Huehnchen).
[1] These authors contributed equally to the present manuscript.

https://doi.org/10.1016/j.nbd.2018.11.017
Received 29 May 2018; Received in revised form 17 October 2018; Accepted 19 November 2018
Available online 22 November 2018
0969-9961/

CD4+ T cells leads to the activation of macrophages and upregulation of adhesion molecules in the blood vessels of peripheral nerves in CIDP (Sainaghi et al., 2010). One subset of those highly pathogenic T cells are T_H17 cells, which were found in CIDP patients with an increased disease activity (Chi et al., 2010). Furthermore, it was demonstrated that T_H17 cells determine disease severity, but not target specificity, in an intercellular adhesion molecule (ICAM)-1 deficient transgenic mouse model of CIDP (Meyer Zu Horste et al., 2014).

An increase of autoimmune disorders in "Western" regions over the last decades have suggested that environmental factors might also play an additional role in the development of autoimmune conditions. It was recently demonstrated that increased concentrations of sodium chloride (NaCl) induce serum glucocorticoid kinase 1 (SGK1), which promotes Interleukin (IL)-23-receptor expression and enhances T_H17 cell differentiation (Wu et al., 2013). Furthermore, murine and human T_H17 cells cultivated under high salt conditions exhibited a highly pathogenic phenotype with an upregulation of pro-inflammatory cytokines such as granulocyte macrophage colony-stimulating factor (GM-CSF), Tumor necrosis factor (TNF)-α and IL-2. Additionally, it was demonstrated that mice kept on a high salt diet show more severe functional and histological characteristics of experimental autoimmune encephalomyelitis (EAE), a common animal model for multiple sclerosis, by augmenting disease progression and infiltration of the central nervous system with immune cells (Kleinewietfeld et al., 2013). These results could be replicated in other autoimmune conditions such autoimmune colitis (Monteleone et al., 2017). Given the parallels between multiple sclerosis and CIDP regarding the pathogenic role of T lymphocytes in the inception of disease, we were interested if a high salt diet would also negatively influence functional, electrophysiological and histological characteristics in a transgenic mouse model of CIDP.

2. Material and methods

2.1. In vivo

Mice of the non-obese diabetic background with knockout of CD86 ($CD86^{-/-}$ NOD) were purchased from Jackson Laboratory (NoD.129S4-Cd86^{tm1Shr}/JbsJ) and thereafter bred at Charité Universitätsmedizin Berlin (Research Department of Experimental Medicine, Berlin, Germany). $CD86^{-/-}$ was confirmed with polymerase chain reaction of tail biopsies prior to the experiments. As it was previously shown that the incidence of autoimmune neuropathy depends largely on the sex with 100% of the female mice developing a CIDP-like phenotype versus only 30% of the males (Salomon et al., 2001), we used female mice only. A total of 22 seven-week old $CD86^{-/-}$ NOD mice were used for this study and all experimental procedures conformed to animal welfare guidelines and were previously approved by an official committee (Landesamt für Gesundheit und Soziales, Berlin, Germany). Animals were maintained on a 12:12 h light/dark cycle and allowed food and water ad libitum. Animals were housed in groups of five to six in an enriched environment. As breeding did not yield a total of 22 female $CD86^{-/-}$ NOD mice of approximately the same age, the experiment was carried out in two subsets with n = 5–6 $CD86^{-/-}$ NOD mice per group at two time points approximately six months apart. We did not check for hormonal activity prior or during the experiment (estrous cycle). The general wellbeing of the mice as well as their weight and disease progression were monitored daily and the clinical symptoms of neuropathy rated using an arbitrary score corresponding to the following definitions: 0 = healthy, 0.5 = light tail weakness, 1.0 = tail paralysis, 1.5 = unilateral hind limb weakness, 2.0 = bilateral hind limb weakness, 2.5 = bilateral hind limb paralysis, 3.0 = unilateral hind limb plegia or fore limb weakness, 3.5 = bilateral hind limb plegia, 4.0 = hind limb plegia and bilateral fore limb paralysis, 4.5 = bilateral hind limb plegia and unilateral plegia of fore limbs, 5.0 = tetraplegia or death due to neurological symptoms. If mice reached a clinical score of > 3.5 AU and had to be sacrificed according to animal welfare guidelines, they were assigned a clinical score of 5 for the remainder of the experiment. Otherwise mice were sacrificed after 30 weeks on the diet independent of their clinical score.

2.1.1. Sample sizes, treatment groups, randomization and blinding

Samples sizes were determined prior to the experiment with G*Power 3 statistical software (Faul et al., 2007) using an α-error of 0.05, a power of 0.8 and a desired effect size of at least f = 0.2 in a 2-way ANOVA testing for the factors "diet" and "time". Animals were assigned to the normal diet containing 0.24% NaCl in food and 0.03% in water (ssniff EF R/M) or high salt diet with 4% NaCl in chow and 1% in water (ssniff EF R/M high sodium, ssniff Spezialdiäten GmbH, Soest, Germany) using unequal block randomization (Graphpad Software, San Diego, CA; https://www.graphpad.com/quickcalcs/randomize1.cfm). The composition of the food pellets regarding fat, protein, carbohydrates, amino acids, vitamins, trace elements and other minerals was identical except for the amount of NaCl. Experimenters were blinded during electrophysiological, histological and statistical analysis.

2.1.2. Behavior analysis

After an acclimatization period of seven days, mice were handled for five consecutive days to familiarize the animals to the investigators. Cages and animals were randomly selected during behavioral assessment, which was carried out in a dedicated laboratory with soundproof chambers. The RotaRod test was used to determine locomotor ability as described previously (Huehnchen et al., 2013). In brief, mice were placed on a rotating rod which gradually increased speed from 4 to 40 rpm in 300 s. The latency to fall off the rod was automatically measured by a floor sensor (TSE Systems GmbH, Bad Homburg, Germany). Mice were trained in the task for four consecutive days and baseline was recorded on the last day. For each mouse, three trials were averaged at each time point.

2.1.3. Nerve conduction studies

Tail nerve sensory conduction velocity (SCV) and sensory nerve action potential (SNAP) amplitudes were measured in ketamine/xylazine anesthesia with a customized Neurosoft Evidence 3102evo ENG device (Schreiber & Tholen Medizintechnik GmbH, Stade, Germany) in antidrome technique as described previously (Boehmerle et al., 2014). Briefly, stimulation needle electrodes were applied at the base of the tail and the recording electrodes placed five cm distal. 50 stimuli of 0.1 ms were applied at supramaximal stimulation intensity and averaged to obtain SNAP and SCV. Sciatic nerve compound motor action potential (CMAP) amplitudes and motor conduction velocity (MCV) were measured in the foot muscles with steel electrodes according to a previously described protocol (Krieger et al., 2014). In brief: the tibial and peroneal nerve were stimulated at supramaximal intensity with needle electrodes at the ankle (distal). Afterwards, the sciatic nerve was stimulated proximal at the sciatic notch. MCV was calculated by measuring the distance between the distal and proximal stimulation electrodes. To obtain F-wave latencies, 10 repetitive supramaximal stimuli were applied proximally at the sciatic notch and the CMAP and F-waves recorded in the foot muscles. To overcome a possible observer bias, the shortest F-wave latency from each mouse was used for statistical analysis.

2.2. Cytokine profiling

Blood samples were drawn in final anesthesia, kept upright for 30 min on ice and centrifuged at 3000 × *g* for 10 min. Serum was snap frozen in liquid nitrogen. Cytokines were analyzed as duplets wherever possible using customized multiplex ELISA plates (Meso Scale Diagnostics, Rockville, MD) according to the manufacturer's protocol. If no data values in either of both technical replicates could be obtained due to the lower limit of the assay's detection range, a lowest positive value of 0.01 pg/ml (= lowest detection range of the assay) was

assigned for this animal and included in the final analysis. To increase statistical power, data from additional control animals from a previous experiment in the same strain and sex and treated under normal diet conditions as well as sacrificed at the same age of 38 weeks (Huehnchen et al., 2018) were included into the current analysis.

2.3. Histology

2.3.1. Immunohistochemistry

Mice were deeply anaesthetized with ketamine/xylazine, decapitated and spleens, lymph nodes, sciatic nerves and dorsal root ganglia extracted and immediately fixed in 4% paraformaldehyde at 4 °C or placed in cryomatrix and frozen in methyl butane at −50 to −60 °C. A series of four to five 20 µm transversal cryosections of the sciatic nerve were cut using a Leica cryostat (Leica Microsystems GmbH, Wetzlar, Germany) and mounted on slides. For staining, slides were rehydrated through a series of graded alcohol baths and rinsed with phosphate-buffered saline (PBS, pH 7.4) and stained with haematoxylin and eosin (HE), Giemsa or Klüver-Barrera according to standard protocols. For immunohistochemistry staining, antigen retrieval was performed for 30 min at 100 °C with 100 mM citrate buffer pH 6.2. Unspecific binding sites were blocked with 10% normal goat serum (NGS) in PBS with 0.1% Triton X-100 (Sigma-Aldrich, Taufkirchen, Germany) prior to incubation with primary antibody (rabbit anti-CD3 (ab5690), mouse anti-CD68 (ab955), both 1:100; abcam, Bristol, UK) at room temperature overnight in 10% NGS followed by incubation with biotinylated secondary antibody (1:250, Life Technologies, Darmstadt, Germany) for 4 h at room temperature in 10% NGS.

2.3.2. Cell counts

Slides were visualized with a Leica SPE confocal microscope (Leica Microsystems GmbH, Wetzlar, Germany) and images of the entire section of the sciatic nerve obtained at x63 magnification using a HCX PL APO glycerin objective and Leica Application Suite software. Images were loaded into Fiji ImageJ software (Schindelin et al., 2012), the area calculated and positive cells manually counted using the cell counter plugin.

2.3.3. Staining intensity analysis

Slides were stained with Luxol Fast Blue to mark myelin. Afterwards images of the transversal sciatic sections in their entirety were obtained at x63 magnification with a Leica SPE confocal microscope equipped with a HCX PL APO glycerin objective using identical settings for bin, exposure and gain. Images were converted to 16-bit grey scale images in Fiji ImageJ software and the grey scale intensity of each pixel measured using the histogram tool, ranging from 0 (darkest) to 256 (lightest). The sum of all pixels in each intensity category (0–50, 50–100, 100–150, 150–200, 200–256 AU) was calculated and expressed as percentage. The percentages of pixels in the 0–50 AU category from one to three sciatic sections of each animal were averaged (Deshmukh et al., 2013).

2.3.4. Teased fiber analysis

Sciatic nerves of approximately 1 cm in length were rinsed in PBS immediately after extraction from the animals and thereafter placed in a solution containing 1% osmium tetroxide in PBS for 1 h at room temperature and afterwards stored in PBS until further processing. Prior to fiber teasing, nerves were placed in a 60% glycerin solution for 1 h at room temperature and thereafter transferred to a 100% glycerin solution and kept overnight at 4 °C. Under light microscopy nerves were gradually teased down to a single axon and afterwards mounted on glycerin/gelatin-coated slides. Images of the sciatic nerve in their entire length were obtained with a Leica SPE confocal microscope equipped with a HCX PL APO glycerin objective at x20 magnification.

2.4. Data processing, availability, exclusion criteria and statistical analysis

The manuscript was written in accordance with ARRIVE guidelines (Kilkenny et al., 2010). Data was analyzed with Prism v6.0 (GraphPad Software, San Diego, CA). Normal distribution of data was checked prior to statistical analysis using Shapiro-Wilk normality test. Normally distributed data was analyzed using unpaired two-sided *t*-tests or 2-way ANOVA with Tukey or Sidak post hoc analysis and is stated as mean ± standard deviation in aligned dot plots. Not normally distributed data or data for which Shapiro-Wilk test failed due to low sample sizes was analyzed with Mann-Whitney-U or Kruskal-Wallis-test with Dunn's method and is presented as median with interquartile ranges in aligned dot plots. 95% confidence intervals (CI) are stated for all tests where appropriate. $p < .05$ was considered statistically significant and is depicted by an asterisk. Only statistical outliers that met Peirce's criterion were eliminated from the data set prior to statistical analysis (Dardis, 2004; Ross, 2003). The dataset generated and analyzed in the present study is available on Mendeley Data (Petra Huehnchen and Wolfgang Boehmerle, High salt diet in CD86−/− NOD mice-OpenData.xls (2018), http://dx.doi.org/10.17632/62pj5hjt63.1).

3. Results

Knockout of the costimulatory molecule CD86 in non-obese diabetic mice ($CD86^{-/-}$ NOD; NoD.129S4-$Cd86^{tm1Shr}$/JbsJ) results in spontaneous development of an autoimmune peripheral polyneuropathy (SAPP) in 100% of female mice by approximately 20 weeks of age (Salomon et al., 2001). We had previously described the main clinical, functional and electrophysiological characteristics of this model (Huehnchen et al., 2018), while others have shown its' immunological and histological features (Quan et al., 2016; Salomon et al., 2001), all of which show great similarity to CIDP.

3.1. Influence of high salt diet on disease progression and locomotor function in $CD86^{-/-}$ NOD mice

Beginning at seven weeks of age, where none of the animals showed signs of autoimmune neuropathy, mice were randomly assigned to a normal diet (ND) or high salt diet (HSD) containing 4% NaCl in food and 1% NaCl in water (Fig. 1A). We observed a significant weight difference at the beginning of the dietary phase: compared to the animals on the normal diet, mice in the high salt group initially lost and then steadily regained weight and afterwards remained on a stable weight level for the remainder of the experimental period (2-way ANOVA, $F_{(1,\ 272)} = 137.8$, $p = .022$ to $p < .001$; Fig. 1B). In contrast, mice on the normal diet initially showed a normal weight gain with aging, but rapidly lost weight with clinical onset of disease. One mouse in the normal diet group and two of the high salt diet mice had to be sacrificed when reaching a clinical score of > 3.5 AU in accordance with animal welfare guidelines. Additionally, one mouse on the high salt diet and two mice in the normal diet group died during anesthesia. The overall survival rate did not differ between groups (Mantel-Cox test, $p = .92$; data not shown). The median clinical score at the end of the experiment was only marginally different between mice on the normal diet (2.5 AU) and the high salt diet (2.25 AU; Fig. 1C). However, mice on the high salt diet showed a significantly delayed onset of neuropathy (ND: 14 weeks, HSD: 18 weeks) and a slower disease progression (50% incidence: ND: 20 weeks, HSD: 23.5 weeks, Mantel-Cox test, $p = .048$; Fig. 1D) corresponding to a shorter duration of clinical symptoms (ND: 11.3 weeks (95% CI 9.4 to 13.3), HSD: 7.8 weeks (95% CI 5.6 to 10.0), unpaired *t*-test, $p = .015$; Fig. 1E). In accordance with the clinical data, locomotor function declined significantly in both groups due to progressive paralysis. However, mice on the high salt diet showed an attenuated loss of motor function over the course of the observational period (28 weeks of ND: 6% of baseline (95% CI 4.8 to 7.2), 28 weeks of HSD: 67% of baseline (95% CI 23.6 to 110.0), 2-way

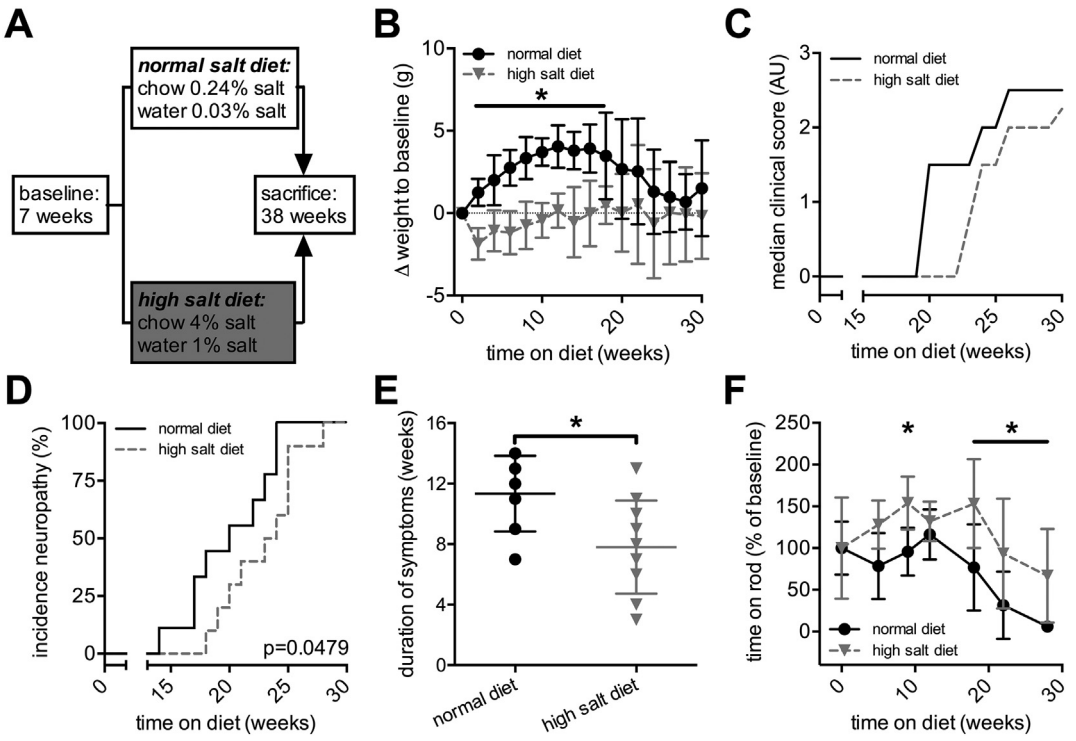

Fig. 1. Effects of high salt diet on clinical course and locomotor function.
(A) Schematic overview of the trial: 7-week old female mice were randomly assigned to a normal diet or high salt diet. Mice were assessed for behavioral and electrophysiological changes at fixed time points and sacrificed after 30 weeks of diet. (B) Mice on the normal diet showed a regular weight gain, but started to lose weight with onset of clinical symptoms. In comparison, mice on the high salt diet remained at a stable weight level throughout the experiment. (C) The median clinical score of neuropathy was not different between groups, but (D) mice on the high salt diet showed a prolonged onset of neuropathy and (E) a shorter duration of symptoms. (F) Mice on the high salt diet showed a prolonged and ameliorated loss of locomotor function. Statistical analysis: (B,F) 2-way ANOVA, (D) Mantel-Cox test, (E) unpaired *t*-test; group sizes (animals): n = 8–11 per group.

ANOVA, $F_{(1,\ 120)} = 38.82$, p = .028; Fig. 1F).

3.2. Electrophysiological characteristics of CD86$^{-/-}$ NOD mice on a high salt or normal diet

We assessed electrophysiological parameters as a more objective measurement of nerve function and disease progression. We observed that the compound motor action potential (CMAP) amplitudes of the sciatic nerve declined in both groups compared to premorbid baseline values (2-way ANOVA, $F_{(1,\ 31)} = 76.07$, p < .001) and was not different between normal and high salt diet at the end of the experiment (p = .50; Fig. 2A). However, while the motor conduction velocity (MCV) decreased in both groups as well over time (2-way ANOVA, $F_{(1,\ 31)} = 59.43$, p < .001), we observed significantly higher MCV values in mice of the high salt diet compared to the normal diet after 30 weeks (ND: 7.5 m/s (95% CI 4.6 to 10.4), HSD: 21.9 m/s (95% CI 9.4 to 34.5), p = .018; Fig. 2B). Similar effects were recorded for the F-wave latency, which increased in both groups compared to baseline (2-way ANOVA, $F_{(1,\ 31)} = 91.10$, p < .001). But again, mice on the high salt diet showed attenuated signs of demyelination, with a significantly less pronounced increase of F-wave latency at the end of the dietary phase (ND: 20.9 ms (95% CI 17.1 to 24.8), HSD: 11.8 ms (95% CI 6.9 to 16.7), p < .001; Fig. 2C). We observed a strong positive correlation between the F-wave latency and the clinical score, underlining the significance of this electrophysiological parameter in predominantly demyelinating neuropathies (linear regression, $r^2 = 0.71$ (95% CI 0.56 to 0.95), p < .001; Fig. 2D).

The sensory nerve action potential (SNAP) amplitude declined significantly only in mice on the normal diet (0 weeks: 47 μV (95% CI 41.8 to 53.3), 30 weeks: 6.1 μV (95% CI -1.8 to 19.9), Kruskal-Wallis-test, p = .003), but not in animals on the high salt diet (0 weeks: 46 μV (95% CI 42.0 to 51.7), 30 weeks: 14 μV (95% CI -0.1 to 46.1), Kruskal-Wallis-test, p = .49; Fig. 2E). The sensory conduction velocity (SCV) decreased in both groups compared to baseline (2-way ANOVA, $F_{(1,\ 30)} = 40.49$, p < .001), but was significantly higher in mice on the high salt diet at the end of the experiment (ND: 11.2 m/s (95% CI 6.3 to 16.2), HSD: 23.2 m/s (95% CI 12.5 to 33.9), p = .029; Fig. 2F).

3.3. Serum cytokine expression in CD86$^{-/-}$ NOD mice under high salt conditions

We next examined cytokine expression in serum samples of mice after 30 weeks on the normal diet or high salt diet. We observed elevated concentrations of Interferon (IFN)-γ (ND: 1.31 pg/ml (95% CI 1.71 to 5.81), HSD: 14.16 pg/ml (95% CI 7.16 to 18.50), Mann-Whitney-*U* test, p = .002, Fig. 3B) and Interleukin (IL)-10 (ND: 20.46 pg/ml (95% CI 23.25 to 95.27), HSD: 106.2 pg/ml (95% CI 85.71 to 136.4), Mann-Whitney-*U* test, p = .040, Fig. 3F) in mice on the high salt diet. IL-17 expression in comparison was significantly decreased in mice receiving the high salt diet (ND: 0.89 pg/ml (95% CI 0.64 to 1.22), HSD: 0.43 pg/ml (95% CI 0.11 to 0.70), Mann-Whitney-*U* test, p = .042, Fig. 3H). No changes of Tumor necrosis factor (TNF)-α, IL-1β, IL-2, IL-6 and IL-12p70 expression were detected in mice of both groups (all Mann-Whitney-*U* test, p = .155 to p > .999, Fig. 3).

3.4. Demyelination and T cell infiltration of peripheral nerves in CD86$^{-/-}$ NOD after high salt diet

Last, we examined histological sections of the sciatic nerve to assess demyelination and immune cell infiltration. We also randomly selected two mice per group for teased fiber analysis. Fiber teasing down to the single axon level revealed swelling and severe demyelination in mice of

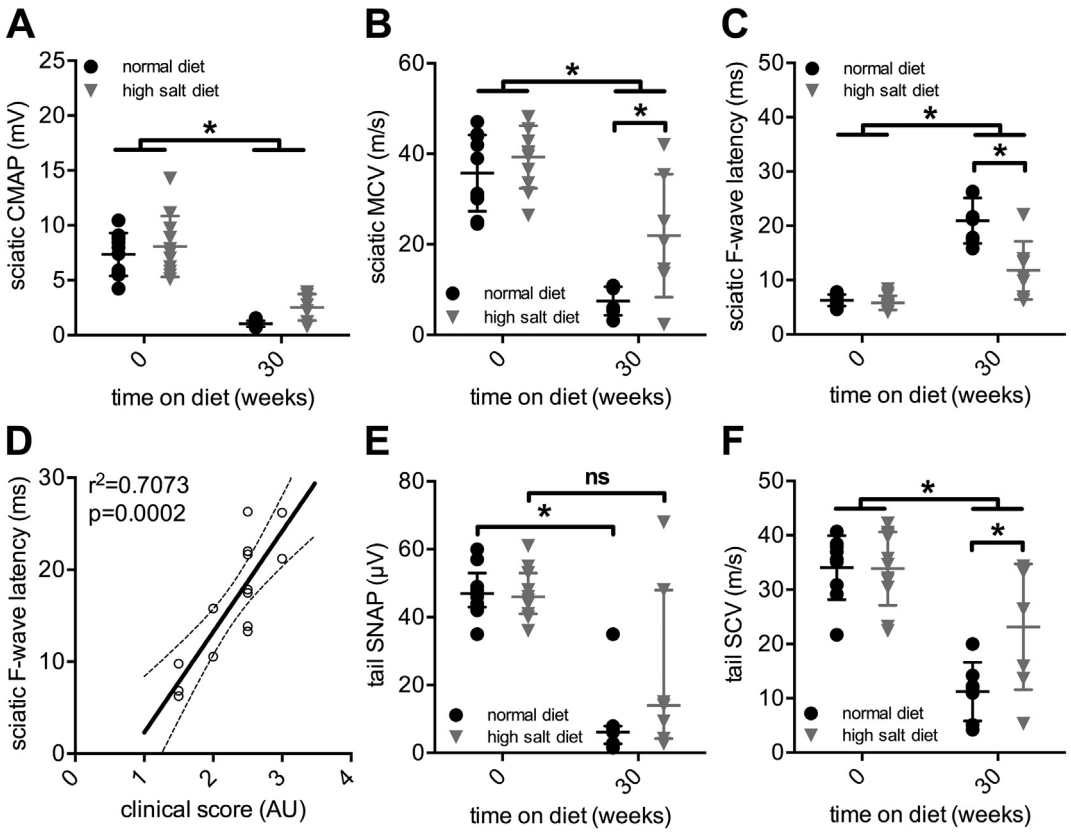

Fig. 2. High salt diet and electrophysiological parameters of autoimmune neuropathy.
(A) In both groups, the compound motor action potential (CMAP) amplitudes decreased over time equally. (B) The motor conduction velocity (MCV) decreased over time in both groups, but mice on the high salt diet showed a higher MCV compared to mice on the normal diet. (C) The F-wave latency increased in both groups with animals on the high salt diet showing an ameliorated pathological increase. (D) The F-wave latency correlated strongly with the clinical score in all samples. (E) Regarding the sensory fibers, the sensory nerve action potential (SNAP) amplitude decreased only in mice on the normal diet. (F) The sensory conduction velocity (SCV) decreased in both groups with mice on the high salt diet showing higher SCV values at the end of the dietary phase. Statistical analysis: (A-C,F) 2-way ANOVA, (D) linear regression analysis, (E) Kruskal-Wallis test; group sizes (animals): n = 7–10 (ND), n = 7–11 (HSD).

the normal diet, while axons from the sciatic nerves of the animals in the high salt group remained mostly compact with reduced demyelination and evenly spaced Ranvier nodes (Fig. 4A). Histological analysis of myelin staining in transverse sections of the sciatic nerves confirmed our clinical and electrophysiological data that mice on the high salt diet had less demyelination compared to mice on the normal diet (ND: 4.8% high intensity pixels (95% CI -0.4 to 8.0), HSD: 7.7% high intensity pixels (95% CI 4.1 to 13.0), Mann-Whitney-*U* test, p = .026; Fig. 4B + C). In addition, mice of the high salt diet group showed a significantly reduced infiltration of the sciatic nerve with immune cells (Fig. 4D). The number of CD3+ T lymphocytes was significantly reduced in histological sections of the sciatic nerves obtained from mice on the high salt diet compared to the normal diet (ND: 1004 cells/mm^2 (95% CI 761 to 1248), HSD: 643 cells/mm^2 (95% CI 380 to 906), unpaired *t*-test, p = .029; Fig. 4E). On the contrary, mice in the high salt diet group showed elevated numbers of CD68+ macrophages in sections of sciatic nerves compared to control mice of the normal diet (ND: 7 cells/mm^2 (95% CI 4 to 14), HSD: 33 cells/mm^2 (95% CI 11 to 56), Mann-Whitney-*U* test, p = .030; Fig. 4F).

4. Discussion

In this study, we analyzed the effects of a high salt diet on disease progression assessed by clinical, behavioral, electrophysiological and histological tests in a transgenic animal model of spontaneous autoimmune polyneuropathy. Amongst others, we had previously shown that this model represents typical features of CIDP (Huehnchen et al., 2018; Salomon et al., 2001). As it was demonstrated that high salt conditions can drive autoimmunity by boosting T_H17 cells (Kleinewietfeld et al., 2013), impairing regulatory T cell function (Hernandez et al., 2015) and increasing the production of pro-inflammatory cytokines (Monteleone et al., 2017), our observation of a *beneficial* effect of the high salt diet was contrary to our initial hypothesis. Intriguingly, onset of clinical symptoms was delayed under high salt conditions and mice showed a slower deterioration of motor function as well as reduced demyelination of peripheral nerves. Furthermore, histologic analysis demonstrated a reduced immune cell infiltration of sciatic nerves. The experiment was done in two subsets with n = 5–6 mice per group each at two different time points following the exact same protocol. We observed similar effects in both subsets of experiments with the second sub-study replicating the previous results. This approach makes an incidental experimental artifact very unlikely. Spontaneous autoimmune polyneuropathy was induced in this animal model by the knockout of the costimulatory molecule CD86 in mice of the non-obese diabetic background. It was previously demonstrated in experimental autoimmune encephalomyelitis (EAE) that the effects of high salt dietary conditions on immune cells and clinical parameters seem to be sex-specific with female mice being more negatively affected by high sodium intake than males (Krementsov et al., 2015). The underlying mechanism of this finding remains unclear, but it has recently been shown that high salt conditions have a strong influence on the gut microbiome by depleting certain bacteria, which seem to modulate T_H17 cells (Wilck et al., 2017). Additionally, a treatment with the "missing" microbiota ameliorated the aggravation of EAE caused by high salt intake. This is an interesting finding, given that the gut microbiota varies largely between the sexes. In the type 1 diabetes mouse

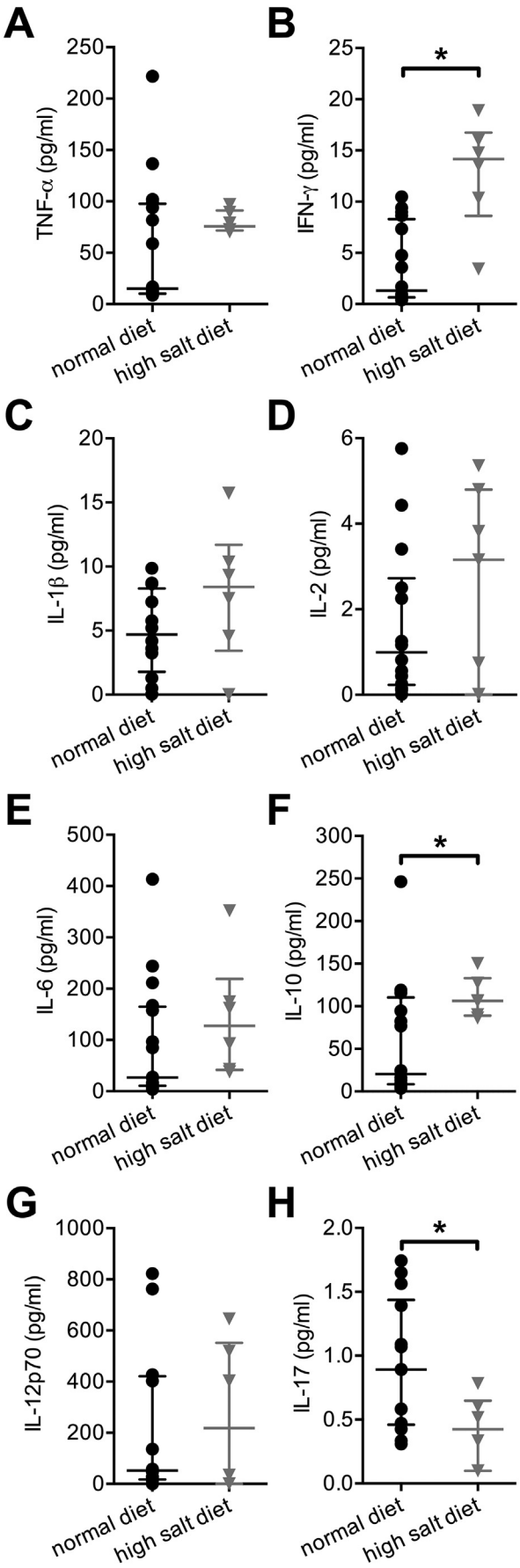

Fig. 3. Effects of a high salt diet on serum cytokine expression.
Serum samples were taken after 30 weeks on the normal or high salt diet. No differences in cytokine levels were observed for (A) Tumor necrosis factor-α (TNF-α), (C) Interleukin (IL)-1β, (D) IL-2, (E) IL-6 and (G) IL-12p70. Mice on the high salt diet showed elevated levels of (B) Interferon (IFN)-γ and (F) IL-10 as well as decreased levels of (H) IL-17 compared to animals receiving the normal diet. Statistical analysis: all Mann-Whitney-*U* test; group sizes (animals): (A,B,E,F) n = 16 (ND), n = 6 (HSD); (C,G) n = 12 (ND), n = 6 (HSD); (D) n = 14 (ND), n = 7 (HSD), (H) n = 14 (ND), n = 6 (HSD).

model for example, it has been shown that a male microbiome has protective effects (Markle et al., 2013). However, in our study we only used female mice and still observed a beneficial effect of hypertonic NaCl conditions. A different finding of Krementsov and colleagues was that the effect of high NaCl seems to be genetically controlled and varies between mouse strains (Krementsov et al., 2015). Therefore, we discussed whether the NOD background of the mice used in our study may have influenced the effects we observed with the high salt dietary conditions. Another study that used animals of the NOD background did also not observe exacerbating effects of a high sodium diet on autoimmunity in a model of autoimmune thyreoiditis (Kolypetri et al., 2014), but beneficial effects were not found either. Additionally, the investigators included other mouse strains and models in their study and did not find any effects of the high salt diet on the occurrence of autoimmune thyreoiditis (Kolypetri et al., 2014). We therefore conclude that a beneficial effect of the high salt conditions solely based on the NOD mouse strain used in our study is unlikely. It rather seems that the effects high sodium concentrations elicit in the immune system are much more diverse than initially expected. Two studies in humans could show that even a short high salt diet with 12–15 g/day induces monocyte expansion and activation (Yi et al., 2015; Zhou et al., 2013) while a decrease in salt intake to < 6 g/day resulted in a reduced production of pro-inflammatory cytokines IL-6 and IL-23 and enhanced the production of the anti-inflammatory cytokine IL-10 (Yi et al., 2015). In vitro studies have shown that treatment of macrophages with hypertonic sodium induces a pro-inflammatory macrophage phenotype, which was accompanied by increased activation of nuclear factor 'kappa-light-chain-enhancer' of activated B-cells (NF-κB) and Mitogen-activated protein kinase-cascade (MAPK) signaling pathways. Transfer of these pathogenic NaCl-conditioned macrophages into EAE-diseased animals resulted in significant disease aggravation compared to untreated macrophages (Hucke et al., 2016). On the other hand, it was also demonstrated by other groups that high NaCl concentrations in the *extracellular* environment were shown to induce an anti-inflammatory M2-like macrophage phenotype (Amara et al., 2016). The latter finding could explain that we found elevated numbers of macrophages in the sciatic nerves of mice on the high salt diet despite overall reduced inflammation. It is also possible, that while hypertonic sodium concentrations potentially lead to an expansion of T_H17 cells, these cells may not always show pro-inflammatory capacities. In fact, it was demonstrated that T_H17 cells which differentiated independently of IL-1β can have regulatory T cell-like properties instead of the pathogenic properties of IL-17/IFN-γ double producing T_H17 cells (Noster et al., 2015; Noster et al., 2016; Zielinski et al., 2012). In our study, we found elevated systemic cytokine levels for IL-10 as well as reduced levels of IL-17 in the mice on the high salt, but also elevated levels for INF-γ. These findings seem to partially underline the hypothesis of a possible differentiation of T_H17 cells with non-pathogenic, auto regulatory properties induced by the high sodium conditions in our model. However, additional studies are needed to further elucidate the underlying mechanisms and to exclude other effects including but not limited to metabolic or hormonal changes due to high salt conditions.

Given the diverse data, it seems clear that high salt dietary conditions cannot automatically be linked to increased autoimmunity. This is underlined by a longitudinal five-year follow-up study of patients with clinically isolated syndrome, which showed that sodium intake was not

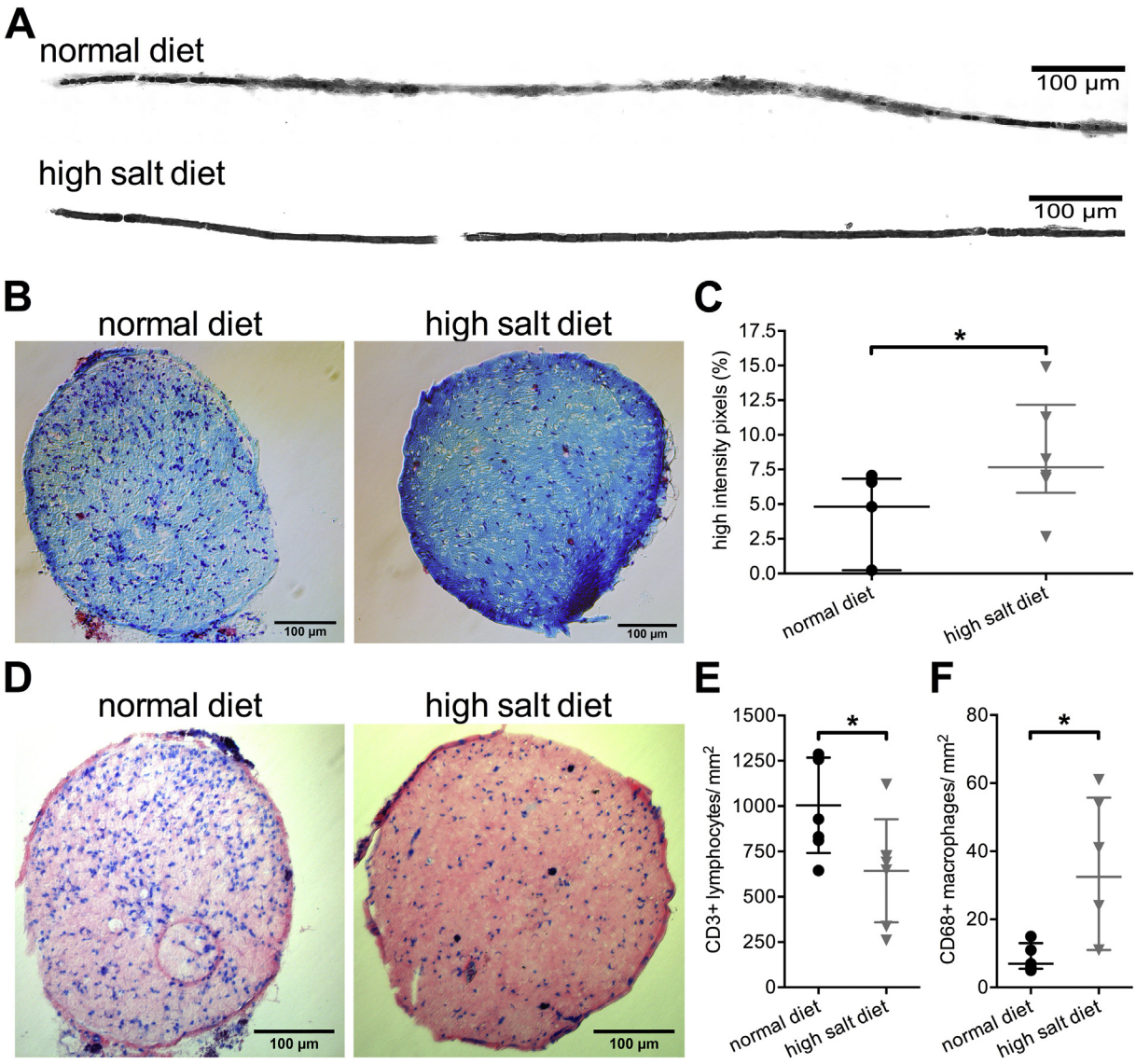

Fig. 4. Histological assessment of peripheral nerves in animals treated with normal and high salt diet.
(A) Representative images of teased fibers from animals of the normal diet (upper panel) and high salt diet (lower panel) group: sciatic nerves of mice on the normal diet showed marked swelling and demyelination, whereas axons of mice on the high salt diet remained mostly intact with reduced demyelination and evenly spaced Ranvier nodes (scale bar 100 µm). (B) Representative images of transversal sections of sciatic nerves stained with Luxol Fast Blue from mice on the normal diet and high salt diet: Mice on the normal diet (left panel) showed more demyelination compared to mice on the high salt diet (right panel) as evidenced by a lighter blue stain (scale bar 100 µm). (C) Mice on the high salt diet showed higher percentages of high intensity pixels in Luxol Fast Blue staining of sciatic nerve sections compared to samples from mice on the normal diet. (D) Representative images of Giemsa staining: Mice on the normal diet (left panel) showed markedly more infiltration of sciatic nerves with immune cells than mice on the high salt diet (right panel) (scale bar 100 µm). (E) Mice of the high salt diet group showed reduced numbers of CD3+ T lymphocytes, but (F) an increased amount of CD68+ macrophages in samples of sciatic nerves compared to animals in the normal diet group. Statistical analysis: (C,F) Mann-Whitney-*U* test, (E) unpaired *t*-test; group sizes (animals): (C,F) n = 5 (ND), n = 6 (HSD), (E) n = 7 in both groups.

associated with clinical or radiological progression to multiple sclerosis (Fitzgerald et al., 2017), contrary to the preclinical results in EAE. Further studies are needed to determine the mechanisms which regulate whether T_H17 cells induced by high sodium conditions drive autoimmunity. Additionally, further (clinical) studies are needed to evaluate the association of sodium intake with disease activity specifically in CIDP.

5. Conclusions

In summary, we demonstrated that high salt diet ameliorates the disease onset and progression as well as the loss of motor function in this transgenic model of a CIDP-like autoimmune neuropathy. Additionally, electrophysiological parameters of demyelination were attenuated in mice on the high salt diet, which was confirmed in histological sections. Furthermore, we observed a reduced immune cell infiltration of the peripheral nerves in mice on the high salt diet.

Conflict of interest

The authors have declared that no conflict of interest exists.

Author contributions

PH, WB and ME designed the study. PH and WB performed the experiments. PH and WB analyzed the data and compiled the figures. PH and WB wrote the manuscript. All authors reviewed the manuscript. ME provided funding for the study.

Acknowledgements

We would like to thank Petra Loge for excellent technical assistance and Dr. Andreas Grützkau as well as Heike Hirseland for access to the mesoscale sector plate reader. This work was supported by the Federal Ministry of Education and Research via the grant Center for Stroke Research Berlin (01 EO 0801) and from the Deutsche Forschungsgemeinschaft (EXC 257 NeuroCure). PH and WB received funding from the Charité Clinician Scientist Program of the Charité Universitätsmedizin Berlin and the Berlin Institute of Health. PH is the recipient of a Rahel-Hirsch fellowship funded by the Charité Universitätsmedizin Berlin.

References

Amara, S., et al., 2016. High salt induces anti-inflammatory MPhi2-like phenotype in peripheral macrophages. Biochem. Biophys. Rep. 7, 1–9.
Boehmerle, W., et al., 2014. Electrophysiological, behavioral and histological characterization of paclitaxel, cisplatin, vincristine and bortezomib-induced neuropathy in C57Bl/6 mice. Sci. Rep. 4, 6370.
Bonin, S., et al., 2018. Cerebrospinal fluid cytokine expression profile in multiple sclerosis and chronic inflammatory demyelinating polyneuropathy. Immunol. Investig. 47, 135–145.
Chi, L.J., et al., 2010. Distribution of Th17 cells and Th1 cells in peripheral blood and cerebrospinal fluid in chronic inflammatory demyelinating polyradiculoneuropathy. J. Peripher. Nerv. Syst. 15, 345–356.
Dardis, C., 2004. Peirce's criterion for the rejection of non-normal outliers; defining the range of applicability. J. Stat. Softw. 10.
Delmont, E., et al., 2017. Autoantibodies to nodal isoforms of neurofascin in chronic inflammatory demyelinating polyneuropathy. Brain 140, 1851–1858.
Deshmukh, V.A., et al., 2013. A regenerative approach to the treatment of multiple sclerosis. Nature 502, 327–332.
Faul, F., et al., 2007. G*Power 3: a flexible statistical power analysis program for the social, behavioral, and biomedical sciences. Behav. Res. Methods 39, 175–191.
Fitzgerald, K.C., et al., 2017. Sodium intake and multiple sclerosis activity and progression in BENEFIT. Ann. Neurol. 82, 20–29.
Hernandez, A.L., et al., 2015. Sodium chloride inhibits the suppressive function of FOXP3+ regulatory T cells. J. Clin. Invest. 125, 4212–4222.
Hucke, S., et al., 2016. Sodium chloride promotes pro-inflammatory macrophage polarization thereby aggravating CNS autoimmunity. J. Autoimmun. 67, 90–101.
Huehnchen, P., et al., 2013. Assessment of paclitaxel induced sensory polyneuropathy with "Catwalk" automated gait analysis in mice. PLoS One 8, e76772.
Huehnchen, P., et al., 2018. Fingolimod therapy is not effective in a mouse model of spontaneous autoimmune peripheral polyneuropathy. Sci. Rep. 8, 5648.
Kilkenny, C., et al., 2010. Improving bioscience research reporting: the ARRIVE guidelines for reporting animal research. J. Pharmacol. Pharmacother. 1, 94–99.
Kleinewietfeld, M., et al., 2013. Sodium chloride drives autoimmune disease by the induction of pathogenic TH17 cells. Nature 496, 518–522.
Kleyman, I., Brannagan 3rd, T.H., 2015. Treatment of chronic inflammatory demyelinating polyneuropathy. Curr. Neurol. Neurosci. Rep. 15, 47.
Kolypetri, P., et al., 2014. High salt intake does not exacerbate murine autoimmune thyroiditis. Clin. Exp. Immunol. 176, 336–340.
Krementsov, D.N., et al., 2015. Exacerbation of autoimmune neuroinflammation by dietary sodium is genetically controlled and sex specific. FASEB J. 29, 3446–3457.
Krieger, F., et al., 2014. Polyethylene glycol-coupled IGF1 delays motor function defects in a mouse model of spinal muscular atrophy with respiratory distress type 1. Brain 137, 1374–1393.
Markle, J.G.M., et al., 2013. Sex differences in the gut microbiome drive hormone-dependent regulation of autoimmunity. Science 339, 1084–1088.
Meyer Zu Horste, G., et al., 2014. Thymic epithelium determines a spontaneous chronic neuritis in Icam1(tm1Jcgr)NOD mice. J. Immunol. 193, 2678–2690.
Monteleone, I., et al., 2017. Sodium chloride-enriched diet enhanced inflammatory cytokine production and exacerbated experimental colitis in mice. J. Crohns Colitis 11, 237–245.
Noster, R., et al., 2015. Two types of human Th17 cells with pro- and anti-inflammatory properties and distinct roles in autoinflammation. Pediatr. Rheumatol. J. 13, O49.
Noster, R., et al., 2016. Dysregulation of proinflammatory versus anti-inflammatory human TH17 cell functionalities in the autoinflammatory Schnitzler syndrome. J. Allergy Clin. Immunol. 138, 1161–1169.e6.
Quan, S., et al., 2016. Regulatory T and B lymphocytes in a spontaneous autoimmune polyneuropathy. Clin. Exp. Immunol. 184, 50–61.
Reynolds, J., et al., 2016. Chronic inflammatory demyelinating polyradiculoneuropathy (CIDP): clinical features, diagnosis, and current treatment strategies. Rhode Island Med. J. 99, 32–35.
Ross, S., 2003. Peirce's criterion for the elimination of suspect experimental data. J. Eng. Technol. 20, 1–12.
Sainaghi, P.P., et al., 2010. The expression pattern of inflammatory mediators in cerebrospinal fluid differentiates Guillain-Barre syndrome from chronic inflammatory demyelinating polyneuropathy. Cytokine 51, 138–143.
Salomon, B., et al., 2001. Development of spontaneous autoimmune peripheral polyneuropathy in B7-2-deficient NOD mice. J. Exp. Med. 194, 677–684.
Schindelin, J., et al., 2012. Fiji: an open-source platform for biological-image analysis. Nat. Methods 9, 676.
Vital, C., et al., 2000. Chronic inflammatory demyelinating polyneuropathy: immunopathological and ultrastructural study of peripheral nerve biopsy in 42 cases. Ultrastruct. Pathol. 24, 363–369.
Wilck, N., et al., 2017. Salt-responsive gut commensal modulates TH17 axis and disease. Nature 551 (7682), 585–589.
Wu, C., et al., 2013. Induction of pathogenic TH17 cells by inducible salt-sensing kinase SGK1. Nature 496, 513–517.
Yi, B., et al., 2015. Effects of dietary salt levels on monocytic cells and immune responses in healthy human subjects: a longitudinal study. Transl. Res. 166, 103–110.
Zhou, X., et al., 2013. Variation in dietary salt intake induces coordinated dynamics of monocyte subsets and monocyte-platelet aggregates in humans: implications in end organ inflammation. PLoS One 8, e60332.
Zielinski, C.E., et al., 2012. Pathogen-induced human TH17 cells produce IFN-[ggr] or IL-10 and are regulated by IL-1[bgr]. Nature 484, 514–518.